LATERAL-LOAD RESPONSE OF A REINFORCED CONCRETE BRIDGE

By Marc O. Eberhard,[1] Member, ASCE, and M. Lee Marsh,[2] Associate Member, ASCE

ABSTRACT: Cyclic, transverse loads were applied to the bents of a three-span reinforced concrete bridge. At a load equal to 45% of the bridge's weight, the bent drift ratio was 0.5%. The bridge's high stiffness was attributed to its continuous superstructure and stiff abutments, which resisted approximately 80% of the applied load. After the soil surrounding the abutments had been excavated, the bridge's stiffness was 15% of the initial stiffness. After the researchers had isolated the bridge superstructure from the abutments, the stiffness was 9% of the initial stiffness. Despite the bents' poor details, damage was limited to yielding of the wingwalls and column cracking; similar bridges should resist likely transverse seismic motions with little damage. The tests provided estimates of the abutment and bent resistances that can be used to evaluate modeling procedures. Following existing modeling procedures, the researchers assembled a model that reflected the measured nonlinear properties of the concrete, steel, soil, bearing pads and polystyrene. The model reproduced the measured response well.

INTRODUCTION

Many bridges are located in seismically active regions of the United States but do not meet current standards for earthquake-resistant construction. Bridge bents built before the mid-1970s are particularly vulnerable to strong earthquakes, and ideally, the responsible agencies would remediate the detailing deficiencies in all old bents. In practice, these agencies can afford to retrofit only the most important bridges and the most vulnerable bents (Lwin and Henley 1993; Roberts 1991).

Identification of the most vulnerable bents in a bridge inventory can be difficult. A bent's vulnerability depends not only on its own stiffness, strength and ductility, but also on the properties of the superstructure, the abutments and the other bents. The properties of the entire structure affect the bent's displacement demand (i.e., the displacement to which a bent is subjected), and in turn, the displacement demand affects the likelihood of flexural failure, splice failure, shear failure, and joint failure (Priestley et al. 1992; Aschheim and Moehle 1992). Unfortunately, little field test data are available to calibrate analytical models of bridge response to large, lateral loads. Although numerous dynamic tests have been performed on bridges (e.g., Crouse et al. 1987; Douglas and Reid 1982), the displacements induced during these tests are orders of magnitude smaller than the displacements likely to occur during strong earthquakes.

This paper discusses the lateral-load response of a three-span reinforced concrete bridge that was constructed in 1966 (Fig. 1). The objectives of the work discussed in this paper were as follows:

1. To develop a method to subject bridges to large, cyclic, transverse loads
2. To measure the stiffness and strength of the bridge
3. To estimate the contribution to resistance the abutments and bents provided
4. To estimate the vulnerability of similar bridges
5. To compare the observed response with that calculated with analytical models

O'Donovan et al. (1994) and Eberhard and Marsh (1997) discuss a second series of tests in which the bents were subjected to drift ratios of up to 3%. Rodehaver (1993) discusses companion small-displacement and dynamic tests.

DESCRIPTION OF BRIDGE

The bridge that was tested (Fig. 1) was located on Interstate 90 in Washington State. It was one of a pair of reinforced concrete bridges that had been slated for replacement by fill because the bridges spanned an abandoned railroad line.

Fig. 2 depicts the bridge in plan and elevation. The 12.2-m wide bridge had two end spans of 12.5 m each and a center span of 18.3 m. The abutments and the bents were skewed by 12.8°. The lateral stiffness of the superstructure was provided

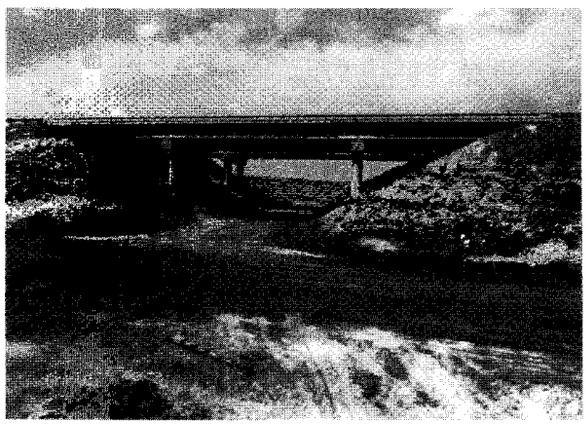

(a)

(b)

FIG. 1. Bridge South Elevation and West Bent

[1]Assoc. Prof., Dept. of Civ. Engrg., Univ. of Washington, Box 352700, Seattle, WA 98195.

[2]Engr., BERGER/ABAM Engrs., Inc., Federal Way, WA 98003.

Note. Associate Editor: Nicholas P. Jones. Discussion open until September 1, 1997. To extend the closing date one month, a written request must be filed with the ASCE Manager of Journals. The manuscript for this paper was submitted for review and possible publication on May 1, 1995. This paper is part of the ***Journal of Structural Engineering***, Vol. 123, No. 4, April, 1997. ©ASCE, ISSN 0733-9445/97/0004-0451–0460/ $4.00 + $.50 per page. Paper No. 10601.

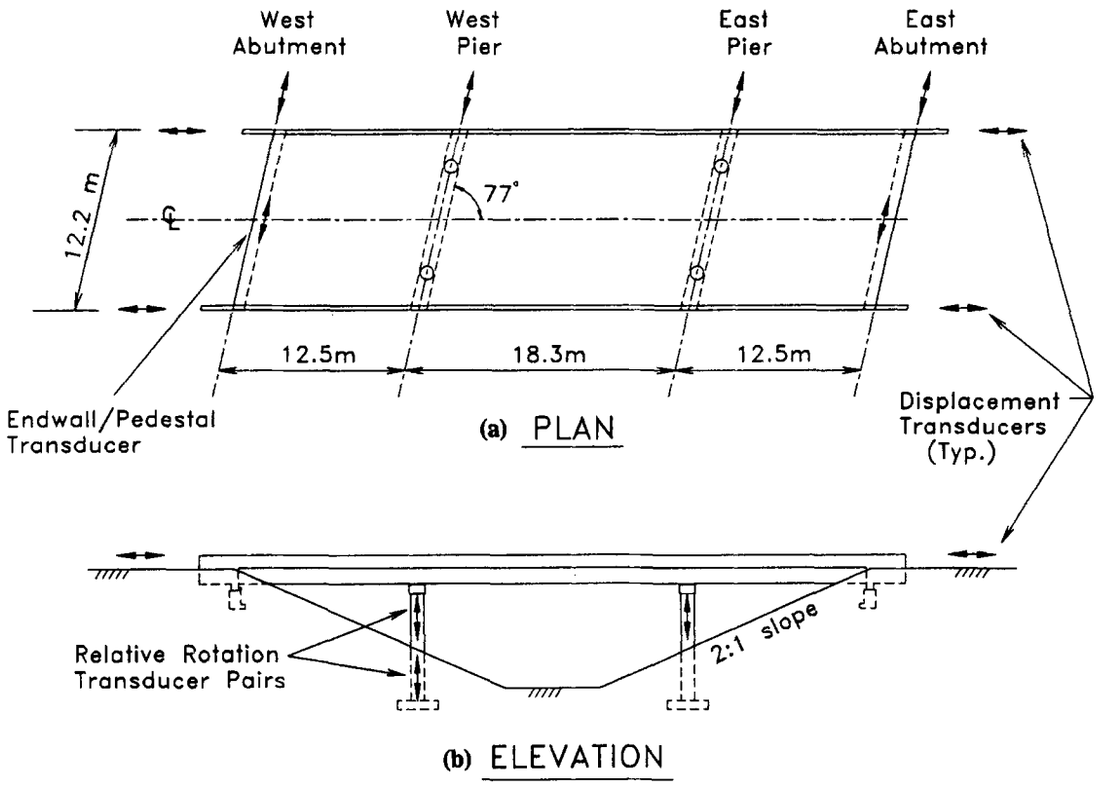

FIG. 2. Bridge Geometry and Instrumentation

mainly by a 165-mm thick, reinforced concrete slab, which was continuous over the two bents. The slab was constructed compositely with six, prestressed concrete I-girders (Fig. 1).

At the bents, the prestressed girders extended 51 mm into 305-mm thick diaphragms, which were heavily reinforced and cast monolithically with the slab. The drop crossbeams were monolithic, with two (914-mm diameter) columns that were supported on 2.9 m by 2.9 m spread footings. The column clear height (crossbeam soffit to top of footing) was approximately 7.6 m, but compacted fill surrounded the lower 3.7 m of the columns. Because the ground surface had a 2-to-1 slope, the soil depth at the footing edges was 4.4 m on the uphill side and 2.9 m on the downhill side. The column longitudinal steel ratio was 1.1%, and the transverse reinforcement consisted of #3 hoops spaced at 305 mm. O'Donovan et al. (1994) provide bent details.

At the abutments, the prestressed girders extended 51 mm into the endwalls (Fig. 3). The endwalls were cast monolithically with wingwalls that extended 2.1 m parallel to the highway. Because the wingwalls were embedded in compacted fill, it was expected that passive soil pressure would resist transverse motion of the endwall. As depicted in Fig. 3, the diaphragm's transverse motion was restrained also by expanded polystyrene and six elastomeric bearing pads (270 × 270 × 22 mm). The polystyrene and bearing pads rested on a concrete pedestal that was supported by a 1.1-m wide footing.

The bridge had deteriorated little during 25 years of service. An inspection revealed only minor cracks and honeycombing.

TEST PROGRAM

Loading History

Six cycles of transverse displacement were imposed to the bents (Fig. 4). The loading was controlled such that the displacements of the bents would be approximately equal.

A preliminary test (test P) was conducted first to check the loading system and instrumentation without damaging the bridge. The following two cycles, denoted as test I, had a target bent displacement of 3.8 mm, which for a clear column height of 7.6 m, corresponded to a drift ratio of 0.05%. In test II, researchers applied the maximum horizontal load that could be applied safely with the loading system, 3,420 kN. This load was approximately equal to 65% of the bridge's weight.

The final two tests Excavated and Isolated (EXC and ISO, respectively) were conducted after the researchers had modified the abutment resistance. Test EXC was conducted after the soil behind the wingwalls and along the abutment endwall had been excavated. After test EXC, the researchers replaced the bearing pads and expanded polystyrene (Fig. 3) with nylon blocks that rested on greased, polished, stainless-steel plates. The nylon block/steel plate support was selected to isolate the bents and superstructure from the abutments. The final cycle, test ISO, was conducted to measure the bents' resistance.

Loading System

The loads were applied to the bents with the apparatus depicted in Fig. 5. In each direction, sixteen 13-mm diameter prestressing strands applied loads to each bent. Each set of strands was pulled by two hydraulic rams that were installed in a jacking frame located at ground level. Reactions were provided by a second set of prestressing strands that was anchored by deadman anchors. In the horizontal plane, all components of the load train were aligned along the 12.8° skew of the bridge. In the vertical plane, components were aligned at an angle of 14° below the horizontal.

Instrumentation

Ten displacement transducers (linear-variable-differential-transformers and Temposonics™ transducers) were installed to monitor displacements of the superstructure (Fig. 2). Eight of these instruments measured horizontal displacements of the superstructure relative to reference posts located 5–7 m from the bridge. Transverse displacements along the skew were mea-

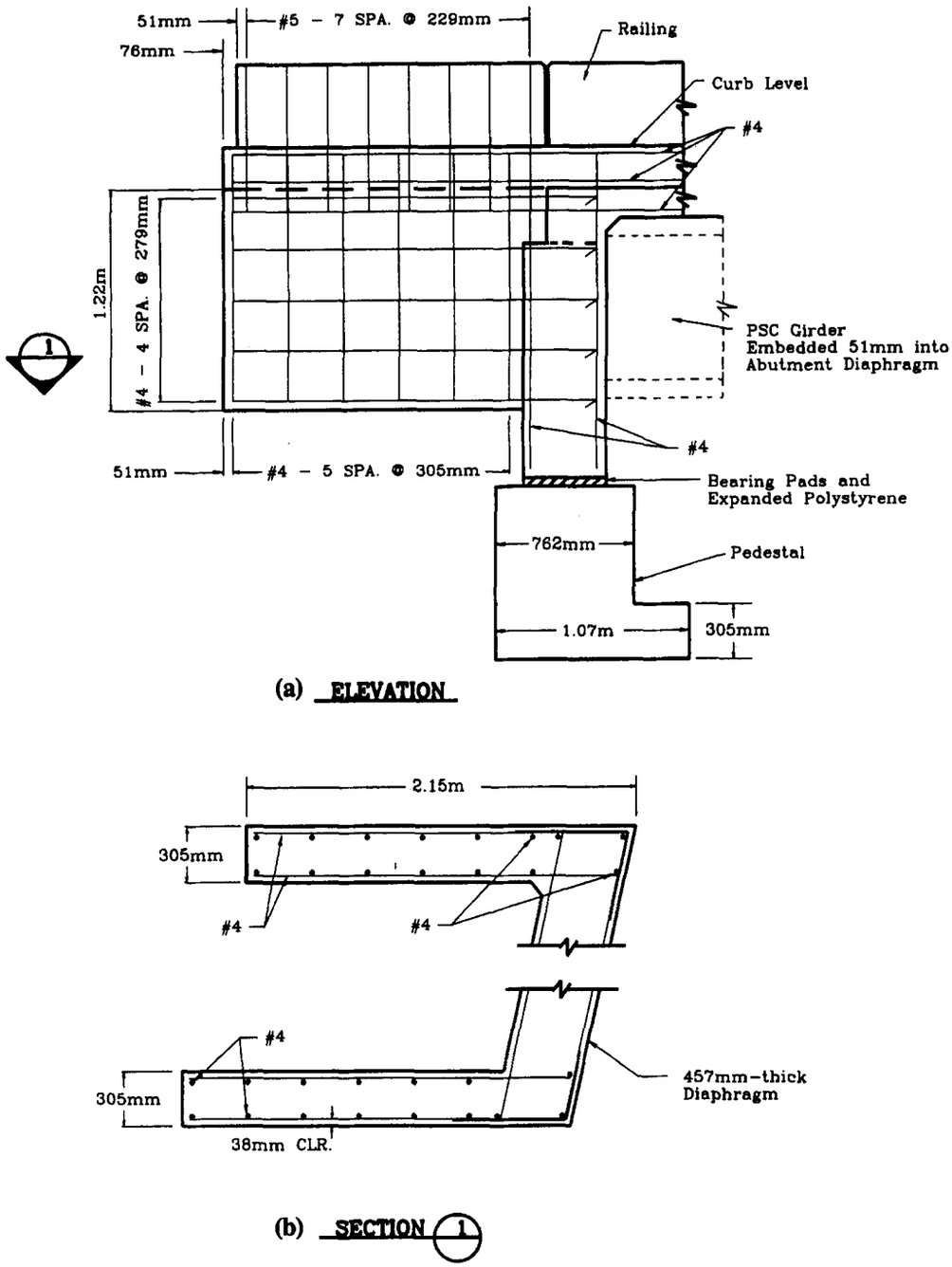

FIG. 3. Abutment Details

sured at each abutment and bent, whereas longitudinal displacements were measured at the abutment only. Each superstructure instrument measured the movement of a weight that was coupled to the bridge by a cable and pulley system. Before the tests were conducted, the accuracy of the instrumentation apparatus was established as approximately ±0.03 mm. Two instruments monitored the relative transverse displacement between the abutment diaphragms and the supporting pedestals (Fig. 3).

Additional instruments measured the relative rotations of critical beam and column cross sections at the bents. To provide access to the base of the west-bent columns, 1-m wide trenches were excavated to the top of the footings. These trenches were oriented perpendicular to the direction of the applied load to minimize the effect of the excavation on the bent's lateral-load resistance. On the east bent, instruments were placed only on the crossbeams and at the top of the columns, and no access trenches were excavated.

The applied loads were determined based on the pressures in hydraulic jacks that had been calibrated before the tests. Eberhard et al. (1993) provide details of the instrumentation.

OBSERVED RESPONSE

To organize the observed response, it is convenient to introduce a naming convention to refer to each half cycle of loading. Each half cycle will be referred to by the test name (P, I, II, EXC or ISO), the direction of applied load (S or N) and the number of times the bridge had been pulled in that direction during the test (1 or 2). For example "half-cycle IIS2" corresponds to the second pull to the south during test II.

For each half cycle, Table 1 lists the average abutment and bent displacements measured between the beginning of each half cycle and the time of maximum load. The corresponding displacement response histories are presented in Fig. 6.

Test P

During test P, the bents were subjected to an applied load of 1,350 kN, which corresponded to approximately 25% of the bridge's weight. The bent displacement was only 1.6 mm, and no new damage was observed during this test.

Test I

In test I, the researchers imposed two cycles of displacement to a drift ratio of 0.05% (Fig. 4). The average maximum applied load for the four cycles (2,500 kN) was equal to 45% of the bridge's weight.

The first flexural crack was found after the maximum load for half-cycle IS1 had been applied. This small crack (less than 0.25-mm wide) was located at the top of the south face of the southeast column. At the same time, researchers observed a small separation between the northwest wingwall and the surrounding soil. After reversing the direction of applied load (IN1), small flexural cracks formed on the north faces of the east columns, and minor crack extension was observed on the northwest wingwall.

During subsequent half cycles (IS2, IN2), no new cracks were found. Existing cracks opened on the column faces that were subjected to tension, and cracks closed completely when the faces were in compression. A small gap formed between the southeast wingwall and the soil.

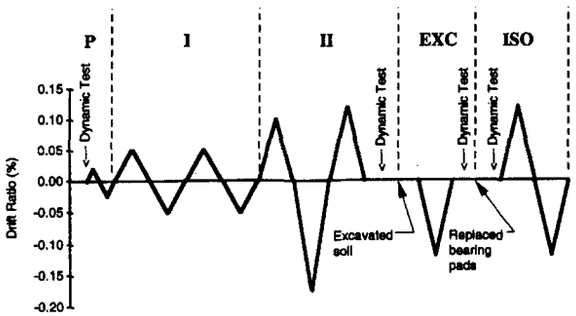

FIG. 4. Imposed Displacement Cycles

Half Cycle IIS1

During half cycle IIS1, the average bent displacement was 8 mm (drift ratio = 0.10%) at the maximum load (3,420 kN). Flexural cracks formed at the tops of all the columns. The largest crack (0.25-mm wide) formed on the south face of the southeast column. Cracks on the northeast and southeast wingwalls opened up slightly more than in previous cycles. Gaps between the north sides of the wingwalls and the soil increased, some of which were as large as 3 mm.

Half Cycle IIN1

During half-cycle IIN1, the bridge lurched northward at the maximum load (3,420 kN), which was equal to 65% of the bridge's weight. Although the applied loads on each bent were nearly equal, the bridge twisted in a counterclockwise direction (as seen from above). The maximum displacement during this half-cycle was 18 mm at the east abutment and 4 mm at the west abutment. After the lurch, the researchers found a 2.5-mm wide crack on the north face of the southeast wingwall, a 0.5-mm wide crack on the north face of the northeast wingwall, and 13-mm gaps between the south faces of the east abutment wingwalls and the surrounding soil. Although some soil separation was observed at the west abutment also, less damage was apparent at the west abutment than at the east abutment. This distribution of damage was consistent with the measured twist of the superstructure.

The amount of cracking and soil disturbances at the bents was larger in half-cycle IIN1 than in previous cycles. Flexural cracks, spaced approximately every 0.3 m, formed in the top 1 m of the east-bent columns. On the west-bent columns, cracking was visible for the top 0.3 m. Nonetheless, the cracks were small. With the exception of a single 0.5-mm wide crack on the southeast column, the column cracks were 0.25-mm wide or less. No cracks were visible at the bottom of any of the columns. The only manifestation of movement of the lower portion of the columns were small separations between the columns and the surrounding soil.

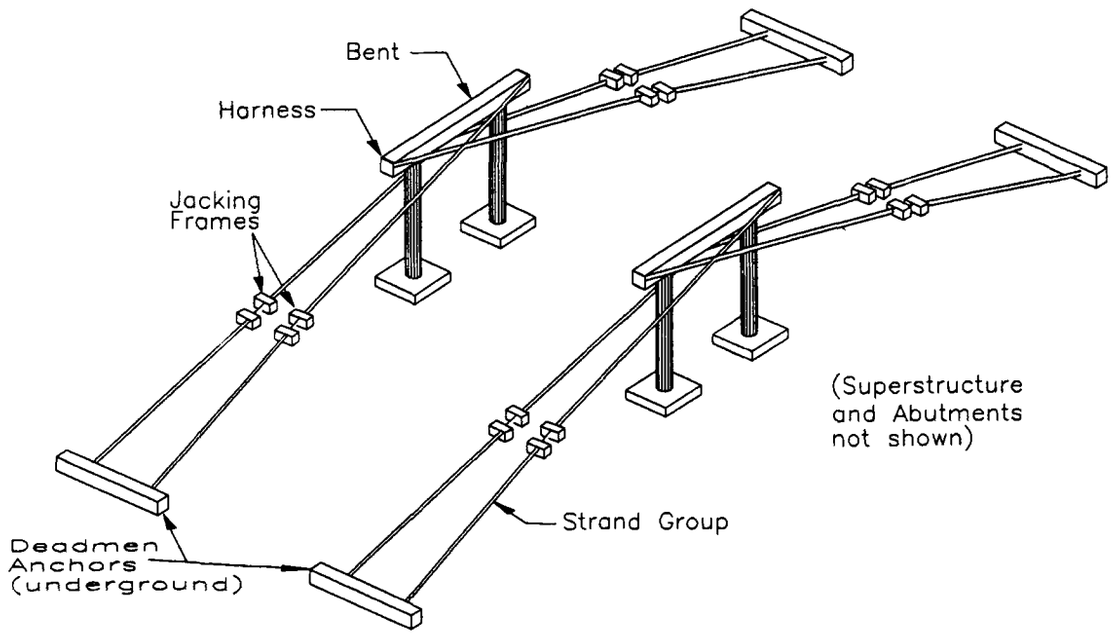

FIG. 5. Loading System

TABLE 1. Response Maxima

Test cycle (1)	Horizontal force (kN) (2)	Average abutment displacement (mm) (3)	Average bent displacement (mm) (4)	Superstructure	
				Deformation (mm) (5)	Recovered deformation (%) (6)
PS1	1,358	0.5	1.6	1.2	—
—	0	−0.4	−1.5	−1.1	92
PN1	−1,348	−0.8	−1.5	−0.7	—
—	0	0.4	1.2	0.8	106
IS1	2,760	1.7	3.9	2.2	—
—	1	−1.8	−3.9	−2.1	96
IN1	−2,711	−1.7	−3.9	−2.3	—
—	0	1.6	3.6	2.1	91
IS2	2,211	2.0	3.9	1.9	—
—	0	−1.3	−3.0	−1.6	86
IN2	−2,384	−1.8	−3.7	−1.9	—
—	0	1.0	2.9	1.9	99
IIS1	3,421	4.8	7.7	3.0	—
—	0	−1.8	−4.7	−3.0	100
IIN1	−3,421	−11.1	−13.8	−2.7	—
—	0	−0.0	3.3	3.4	124
IIS2	3,421	13.2	16.1	2.9	—
—	0	−1.8	−4.9	−3.0	105
EXCN1	−1,555	−11.3	−11.9	−0.6	—
—	0	0.8	2.0	1.2	189
ISOS1	967	12.2	12.2	0.1	—
—	0	−10.8	−10.8	−0.0	86
ISON1	−897	−12.5	−12.6	−0.1	—
—	0	10.0	10.3	0.3	306

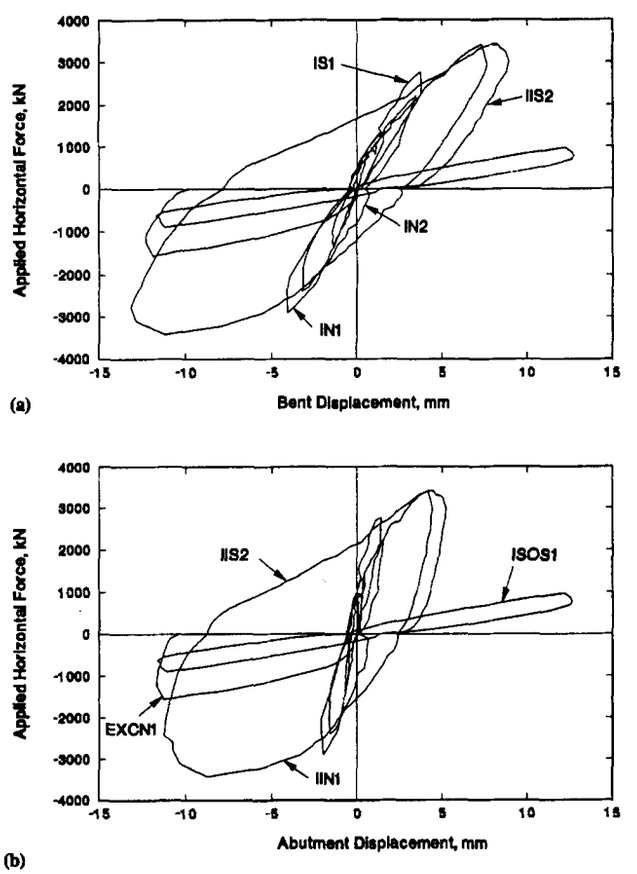

FIG. 6. Measured Response Histories

Half Cycle IIS2

The damage observed during half cycle IIS2 was similar to that observed during IIN1. No new cracks were reported in the columns, but new cracks formed in the abutment wingwalls. At the east abutment, cracks formed on the south face of the wingwalls. The soil gaps behind the wingwalls closed on the south faces, and new soil gaps opened to approximately 13 mm on the north faces. At the west abutment, only minor cracking was observed, and the soil gaps were smaller than at the east abutment.

Test EXC and ISO

After removing the soil behind the wingwalls and along the endwalls, the researchers subjected the bridge to one half cycle of displacement (test EXC). A horizontal load equal to 30% of the bridge's weight produced abutment and bent displacements that were similar to those of test II. After the bearing pads and polystyrene had been replaced with the low-friction isolation system, the maximum load (at similar displacements) was less than 20% of the bridge's weight.

Column Curvatures

Fig. 7 reports the average curvatures at the top of the northwest columns for each half cycle at the time of maximum applied load. The curvatures were computed based on relative rotations of adjacent beam section located 0, 75, 380, and 685 mm from the crossbeam soffit. On the basis of the measured strength of concrete cores (44 MPa) and a rupture modulus of $0.6\sqrt{44}$, the cracking curvature was estimated as 5×10^{-5} rad/m. As shown in Fig. 7, the northwest column exceeded the cracking curvature for the first time during test I. The measured curvatures were consistent with the observed cracking.

RELIABILITY OF MEASUREMENTS

Because it was impossible to repeat the tests, the researchers investigated the measurement reliability by checking for internal consistency. For example, the measured transverse motion of the abutments was corroborated by the two instruments that measured relative displacement between the abutment endwall and the pedestal (Fig. 2). These instruments consistently recorded displacements that were approximately 90% of the abutment displacement relative to the reference posts.

Another opportunity to check for internal consistency was the computed superstructure deformation, which was calculated as the average bent displacement minus the average abutment displacement. As shown in Fig. 8, superstructure deformation varied linearly with the applied load for test P, I, and II. Such a linear relationship is reasonable because the force-deflection relationship for the superstructure likely remained linear, and the transverse superstructure shear was approximately proportional to the applied load. The shear was proportional to the applied load because the bents were relatively flexible and their force-deflection relationships likely remained

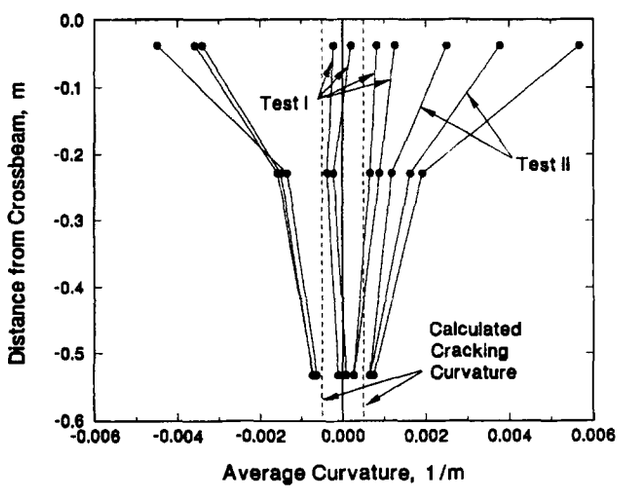

FIG. 7. Curvatures at Maximum Loads for Northwest Column

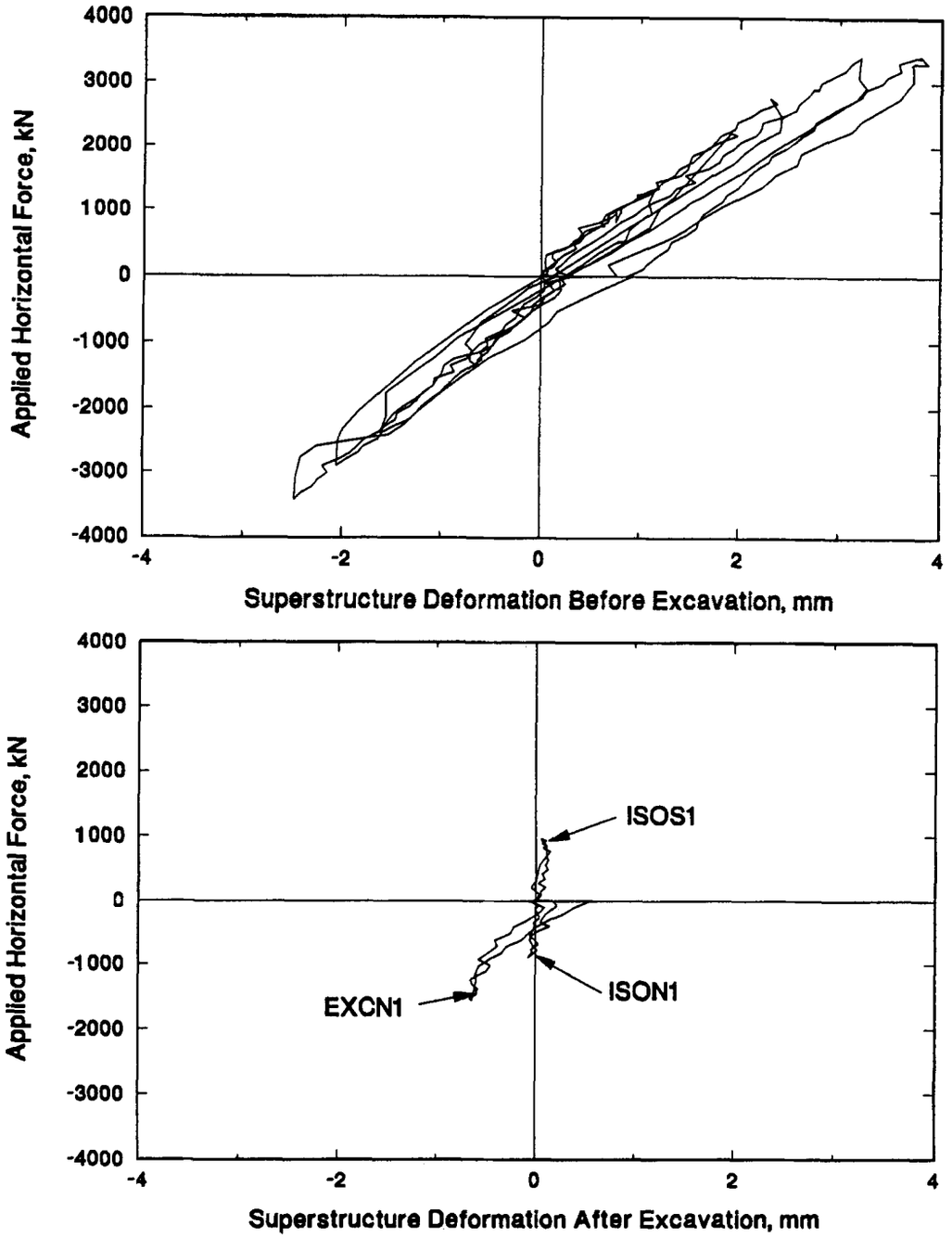

FIG. 8. Superstructure Deformation History

nearly linear. As expected, the superstructure deformation after excavation (test EXC) was smaller than in previous tests because the excavation had reduced the abutment resistance. The superstructure deformation was negligible after isolation (test ISO) because the abutment resistance was negligible.

VARIATION IN BRIDGE STIFFNESS

Large variations in stiffness are apparent in the response histories (Fig. 6). To quantify the stiffness decreases for each test, effective stiffness (Fig. 9) were computed based on the maximum load and displacement at the points of maximum load (Table 1). The bridge's initial stiffness was 900 kN/mm, but it decreased to 77% of the initial stiffness during two cycles to a drift ratio of 0.05% (test I). The effective stiffness decreased further (to 41% of the initial stiffness) during the cycles in which the wingwalls were damaged (test II). After the soil surrounding the abutments had been excavated (test EXC), the residual stiffness was only 15% of the initial stiffness.

The measured effective stiffness during test ISO was only 11% of the initial stiffness. The bent's actual stiffness was even smaller than this value because the measured stiffness included the resistance provided by the abutment isolation system. As discussed by O'Donovan et al. (1994), the isolation system provided a resistance of approximately 80 kN. The corrected bent stiffness was only 9% of the bridge's initial stiffness.

COMPONENT RESISTANCES

The bent and abutment stiffnesses could not be determined uniquely from test I because the bridge was indeterminate. Nonetheless, by comparing the response of the bridge in test

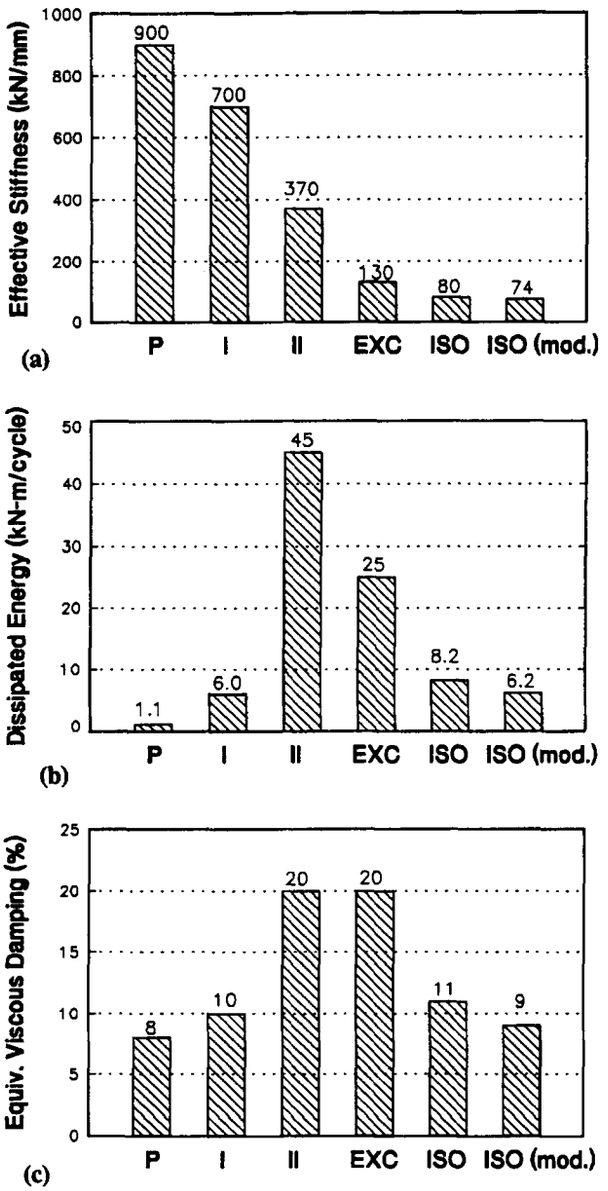

FIG. 9. Stiffness and Energy-Dissipation Characteristics

I with the responses in tests EXC and ISO, it was possible to estimate the resistances provided by the bents, abutment soil, bearing pads, and polystyrene. Such estimates are helpful in understanding the behavior of the bridge and in calibrating analytical models.

On the basis of the results of test ISO, the bent stiffness (adjusted for the effect of the abutment isolation system) was found to be approximately 74 kN/mm. Therefore, during test I, when the columns were less cracked and the soil was elastic, it would be reasonable to assume that the bent stiffness was in the range of 100–150 kN/mm.

Between cycles EXCN1 and ISON1 (Fig. 6 and Table 1), it is unlikely that the bent stiffness changed significantly because the bents had been subjected to similar displacements in test II. Based on a comparison of the response histories in these two cycles, it appears that the bearing pads and polystyrene at the two abutments contributed a force of approximately 600–700 kN before they slipped. Considering that the vertical reaction at each abutment was approximately 800 kN, this slip force corresponded to coefficient of friction for the bearing pad/polystyrene combination of 0.38 to 0.42. After slip the excavated tangential stiffness was the same as the isolated stiffness. This observation was corroborated by the superstructure deformation measurements. During the latter portion of half-cycle EXCN1 (loads exceeding 1,000 kN), the slope of the applied force-superstructure deformation curve was similar to the slope of the corresponding ISO curve (Fig. 8).

The estimate of the abutment soil resistance during test I is indirect. At an average load of 2,500 kN, the average bent displacement was 3.9 mm (Table 1). If the bent stiffness was 100–150 kN/mm, then the bents provided a resistance of 400–600 kN. If the bearing pad and polystyrene properties remained constant during the test, they likely resisted an additional 600–700 kN. Therefore, based on the remaining force of 1,200–1,500 kN and the measured abutment displacement of 1.7 mm, the likely soil stiffness was 700–900 kN/mm. Therefore, during test I, the bents resisted approximately 20% of the applied load, the bearing pads and polystyrene resisted approximately 25% of the load, and the soil resisted approximately 55% of the load.

SEISMIC VULNERABILITY

The measured bent force-displacement response, combined with the observed damage, provided information with which to estimate the bridge's vulnerability to transverse components of ground motion. To make this estimate, it is necessary to consider the energy-dissipation characteristics of the bridge.

Equivalent Viscous Damping

Large variations in the bridge's energy-dissipation characteristics are apparent in Fig. 6. To quantify these variations, the bent force-displacement response was integrated to obtain the energy dissipated per loading cycle (Fig. 9). Most of the energy was dissipated during test II (1½ cycles at 45 kN·m/cycle) and test EXC (½ cycles at 25 kN·m/cycle).

However, it is misleading to consider dissipated energy only in quantifying the energy-dissipation characteristics of the bridge because the imposed displacements varied greatly among the tests. A nondimensional measure of the energy-dissipation characteristics of a system is the equivalent viscous damping ratio, ζ, which is computed by equating the energy dissipated by a nonviscous system with that dissipated by an equivalent viscous system. For a system subjected to resonant harmonic motion, the equivalent viscous damping can be expressed as follows:

$$\zeta = \frac{E_d}{2\pi k A^2} \tag{1}$$

where E_d = energy dissipated per cycle (Fig. 9), k = effective stiffness (Fig. 9), and A = displacement amplitude (Fig. 6) (Clough and Penzien 1993).

As shown in Fig. 9, the equivalent viscous damping ratio was equal to 20% for tests II and EXC. For the other cycles, the damping ratio varied from 8 to 10%. However, one note of caution is warranted, the damping likely to occur during an earthquake might differ from that observed in the static tests because the loading rates differed. A half cycle of loading lasted up to 2 h, whereas a half cycle of motion during an earthquake might last only 0.1 s. More creep, and hence, more energy dissipation would occur during the static tests. On the other hand, radiation damping would tend to dampen the bridge's dynamic response during an earthquake.

Effective Peak Acceleration

The bridge's transverse response during an earthquake can be estimated by treating the bridge as a single-degree-of-freedom (SDOF) system (such a simplification is reasonable because the superstructure deformation was small). Accordingly,

the weight of the system was taken as the bridge weight (5,300 kN), and the effective stiffnesses were derived from the tests (Fig. 9). The resulting effective period for test I was 0.17 s. During this test, the applied load was equal to 45% its weight. Allowing for a dynamic amplification factor of 2.5 (*AASHTO* 1994), which is conservative for a damping ratio of 8% and the computed period, this level of base shear demand (and the associated damage) corresponds to an effective peak acceleration of 0.2 g. During test I, damage was limited to minor column cracking.

The wingwalls yielded at an applied load equal to 65% of the bridge weight (test II). Allowing again for a dynamic amplification factor of 2.5, the bridge would likely resist an 0.3 g ground motion without significant inelastic action. The ductility capacity observed after the wingwalls yielded suggests that the bridge could sustain a global ductility demand of two, with only moderate damage to the wingwalls. Therefore, the bridge would likely sustain little damage even if the transverse effective peak acceleration were as high as 0.5 or 0.6 g.

The extent to which behavior of the test bridge can be confidently extrapolated to other bridges depends on their similarity. The continuous superstructure of this bridge transmitted the applied forces to the abutments; such a load path does not exist for many simply-supported bridges. The resistances provided by the polystyrene and soil at the abutment depend on the abutment configuration. For example, if the shear keys in a seat-type abutment fail, the abutment would not transmit the superstructure transverse shear to the wingwalls, and the piers would undergo larger displacements. In addition, the bent's force-displacement response will vary depending on the column height and the height of the soil surrounding the columns.

ANALYTICAL MODEL

Nonlinear models were created for the bridge in its initial, excavated, and isolated conditions. The models accounted for the expected nonlinear behavior of the columns, wingwalls, soil, bearing pads, polystyrene, and isolation system. The nonlinear analyses were implemented by combining a Basic program with a series of linear analyses (Wilson and Habibullah 1989). A typical finite-element model is shown in Fig. 10, and Eberhard et al. (1993) give the model details.

Reinforced Concrete Elements

Initial properties of the reinforced concrete sections were calculated from the gross section dimensions and an elastic modulus of 32,000 MPa. The elastic modulus was derived from the mean compressive strength of twelve concrete cores (44 MPa) that were taken from the four columns. This measured compressive strength exceeded the specific strength by 60%.

Beam elements modeled the girders, crossbeams, curbs, and columns. Of these members, only the column properties varied during the analyses. When the moment in a column element exceeded the cracking moment (645 kN·m), the moment of inertia in that element was decreased from the calculated gross section value (0.037 m^4) to the cracked value (0.012 m^4).

Shell elements modeled the bridge slab, end diaphragms, and wingwalls. Of these elements, only the wingwall properties varied with increasing load. The wingwall was assumed to remain linear until the point at which it yielded at the interface between the wingwall and the abutment diaphragm. On the basis of the wingwall dimensions and the measured yield stress of two steel coupons (350 MPa), the moment capacity of each wingwall was estimated as 125 kN·m.

Soil along Column

Four linear springs at 3-ft intervals simulated the soil resistance around the columns. The soil's engineering properties were determined from laboratory tests of samples that were collected at the site. The in-situ unit weight of the soil was 14 N/m^3, and its dry unit weight was 12.5 N/m^3. By comparison, typical dry unit weights for silty sands range from 11 N/m^3 to 16 N/m^3 (Kulhawy and Mayne 1990). On the basis of its unit weight, the soil would be characterized as having medium density. The researchers also performed undrained triaxial tests. On the basis of the measured angle of internal friction (38°), the soil would be classified as dense (O'Neill and Murchison 1983).

Based on these soil properties, stiffnesses were calculated following a p-y curve approach proposed by O'Neill and Murchison (1983) for laterally loaded piles in sands. According to them, the resistance of the soil is a function of the depth below the ground surface, the displacement of the column at that

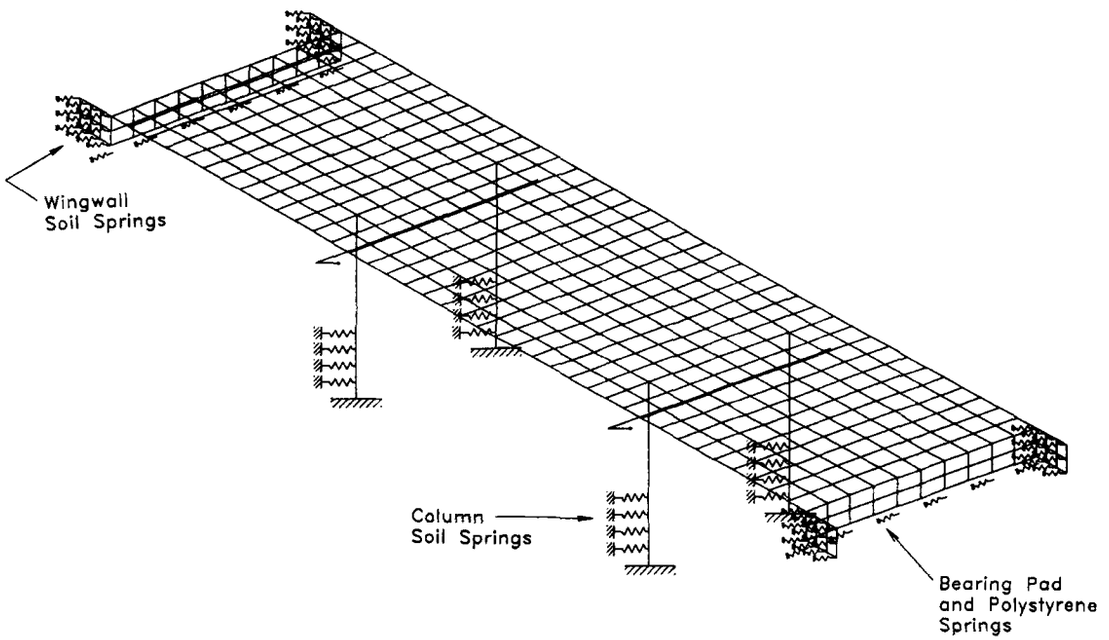

FIG. 10. Finite-Element Model

depth, the ultimate soil resistance at that depth, and the internal angle of friction of the soil.

Abutment Soil

Frictional resistance generated by the soil behind the abutment endwalls was modeled as perfectly plastic. Following a procedure proposed by Fang (1991), the coefficient of friction between sand and concrete was estimated as 0.6. Combining this coefficient with the measured unit weight of the soil and an assumed coefficient of earth pressure (1.0), the resistance was estimated as 160 kN per abutment.

Linear springs modeled the soil resistance behind the wingwalls and perpendicular to each end diaphragm. To model the soil, the researchers followed recommendations proposed by Bowles (1988). For a medium-dense silty sand, Bowles suggested that a typical value for the modulus of subgrade reaction is 48 MN/m^3. Soil spring stiffness for both the wingwalls and endwalls were computed for this modulus. To verify the adequacy of a linear model for the soil behind the wingwall, the soil pressure necessary to yield the wingwalls was estimated. Assuming uniform soil pressure, the computed pressure (75 kPa) was only 30% of the capacity (240 kPa) calculated following the California Department of Transportation procedure for well-compacted backfills (*Bridge* 1994).

Bearing Pads and Polystyrene

The girders transferred the vertical shear into the endwalls, which in turn were supported on pedestals by bearing pads and polystyrene. The shear force-displacement response of the bearing pads and polystyrene was modeled as elastoplastic. To estimate their lateral-load resistance, it was necessary to measure the component's axial and shear force-displacement responses. Laboratory tests were performed for bearing pads that were recovered from the bridge. The polystyrene tests were performed on new samples of polystyrene because the polystyrene from the bridge had not been recovered.

The measured axial-force responses of the bearing pads and polystyrene were nearly linear for strains below 0.035. The compressive elastic modulus was approximately 15 MPa for the bearing pads and 4 MPa for the polystyrene. Consequently, if one neglects the influence of creep, temperature and possible deviations from the specified material thickness, the polystyrene may have carried as much as 75% of the abutment reaction. However, the actual load carried by the polystyrene may have been considerably smaller than 75% if the polystyrene experienced creep during its 25 years of service.

Shear force-displacement behavior for the six bearing pads was measured for the minimum (fully effective polystyrene) and maximum axial stresses (no polystyrene). Within this range of stresses, the shear modulus of the bearing pads was approximately 1.4 MPa, and the reinforced concrete/bearing pad interface was found to have a coefficient of friction of 0.8. Both the bearing pad stiffness and slip (at a load of 150 kN) were modeled. A good approximation of the shear modulus of the polystyrene was 3.2 MPa, and its coefficient of friction was estimated as 0.6. Based on these measurements, one would estimate that the force necessary to overcome the polystyrene friction at each abutment would be 370 kN. Therefore, the total resistance provided by the bearing pads and polystyrene would have been 520 kN.

However, by comparing tests ISO and EXC, it was determined that the total force generated by both the bearing pads and polystyrene was approximately 350 kN. The polystyrene properties appeared to be the most likely source of the discrepancy because the polystyrene that was present in the bridge had not been tested, and in addition, friction is highly sensitive to surface conditions. To reconcile the discrepancy between the measured and computed responses, the polystyrene coefficient of friction was halved.

Isolation System

The isolation system was modeled (test ISO) as perfectly plastic. On the basis of a measured coefficient of friction of

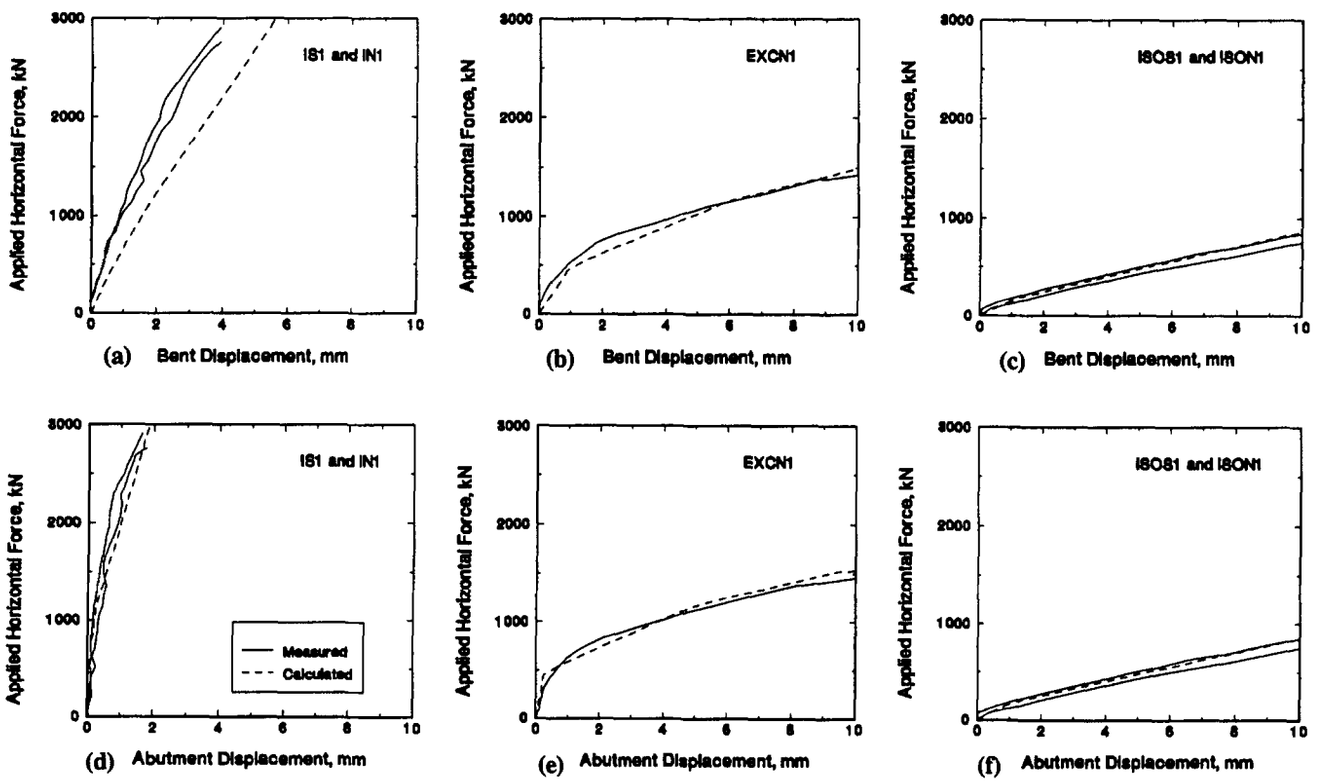

FIG. 11. Comparison of Measured and Calculated Responses

0.05 for the isolation system and an estimated vertical force of 800 kN, the resistance provided by the isolation system was estimated as 40 kN per abutment.

COMMENTS ON ANALYSIS

The calculated response for the model for the bridge in its initial state reproduced the measured response well, particularly at the abutments (Fig. 11). For test I, the calculated abutment load-displacement slopes were within 7% of the measured values, and the model bent load-displacement slopes were within 25% of the measured slopes. An even better fit of the bent response would have been obtained if the researchers had reduced the soil spring stiffnesses behind the endwall. Such a reduction would have been reasonable because the soil tensile capacity was small. The largest discrepancy was the extent of column cracking; minor cracking was observed in the test I, but it was not reproduced by the model.

The model also predicted the maximum lateral-force resistance well (test II). The wingwalls forces in the model reached their strength at an applied load of approximately 3,300 kN, which was nearly identical to the observed failure load of 3,400 kN (test IIS1). As shown in Fig. 11, the measured and calculated responses were nearly identical for both tests ISO and EXC.

CONCLUSIONS

The work presented in this paper led to the following conclusions.

1. In-situ destructive testing is reasonable means of quantifying the large-displacement behavior of a bridge and its components. Field tests do not suffer from some of the constraints imposed by laboratory research, such as the difficulty of reproducing boundary conditions and component sizes.
2. In its undisturbed state, the bridge was stiff and strong. At a bent drift ratio of 0.05%, the bridge resisted a force equal to 45% of its weight. The corresponding effective period was 0.17 s. The bridge resisted a force equal to 65% of its weight with only moderate damage to the wingwalls and minor cracking in the bent columns.
3. The bridge's high stiffness and strength was a consequence of the configuration and construction details of the superstructure and abutments. In the bridge's initial stage, the bents resisted approximately 20% of the applied forces, the bearing pads and polystyrene resisted approximately 25% of the load, and the soil at the abutments resisted approximately 55% of the load.
4. The combination of a continuous superstructure and the large abutment resistance made this bridge sufficiently stiff and strong to resist strong transverse motions without large bent displacements. Longitudinal motions would also be resisted easily by the abutments. Therefore, despite detailing deficiences, the bent vulnerability would be small for likely ground-motion intensities. Bridges that are similar to the test bridge should be assigned a low priority for retrofit.
5. The model presented in this paper reproduced the measured abutment and bent responses well for the bridge and its initial, excavated, and isolated conditions. In this study, soil stiffnesses for the wingwalls were calculated using a tabulated modulus of subgrade reaction. The soil resistance at the columns was modeled as if the column were a pile. The bearing pads and polystyrene were modeled as elastoplastic.
6. It would difficult to reproduce the response well with linear models because some bridge components have nonlinear force-deflection relationships, even for relatively small loads. Column cracking, bearing pad resistance, polystyrene resistance, soil friction, and soil compression are examples of such nonlinear phenomena. However, to model nonlinear behavior well, it is necessary to measure (or estimate) more material properties than are necessary to assemble linear models.

ACKNOWLEDGMENTS

G. Hjartarson and T. O'Donovan conducted the field tests as part of their Master's thesis work at the University of Washington. J. MacLardy performed the finite-element analyses. The research was funded primarily by the Washington State Department of Transportation and the Federal Highway Administration. H. Coffman and E. Henley served as the WSDOT technical contacts. The National Science Foundation provided funding to support undergraduates S. Clark, R. Mah, and C. Wang. T. O'Donovan was supported by the U.S. Army, and G. Hjartarson was supported by the Valle Foundation at the University of Washington.

APPENDIX. REFERENCES

AASHTO LRFD bridge design specifications. (1994). American Association of State Highway and Transportation Officials, (AASHTO), Washington, D.C.

Ascheim A., and Moehle, J. P. (1992). "Shear strength and deformability of RC bridge columns subjected to inelastic cyclic displacements." *Rep. No. UCB/EERC-93/04*, Earthquake Engrg. Res. Ctr., Univ. of California, Berkeley.

Bowles, J. E. (1988). *Foundation analysis and design*, 3rd Ed., McGraw-Hill Book Co., Inc., New York, N.Y.

Bridge design aids manual. (1994). California Department of Transportation, Sacramento, Calif.

Clough, R. W., and Penzien, J. (1993). *Dynamics of structures*, 2nd Ed., McGraw-Hill Book Co., Inc., New York, N.Y.

Crouse, C. B., Hushmand, B., and Marti, G. R. (1987). "Dynamic soil-structure interaction of a single-span bridge." *Earthquake Engrg. and Struct. Dynamics*, 15(6), 711–729.

Douglas, B. M., and Reid, H. R. (1982). "Dynamic tests and system identification of bridges." *J. Struct. Div.*, ASCE, 108(10), 2295–2312.

Eberhard, M. O., MacLardy, J. A., Marsh, M. L., and Hjartarson, G. (1993). *Tech. Rep. WA-RD 305.2*, Washington State Dept. of Transp., Olympia, Wash.

Eberhard, M. O., and Marsh, M. L. (1997). "Lateral-load response of two reinforced concrete bents." *J. Struct. Engrg.*, ASCE, 123(4), 461–468.

Fang, H. Y. (1991). *Foundation engineering handbook*, 2nd Ed., Van Nostrand Reinhold, New York, N.Y.

Kulhawy, F. H., and Mayne, P. W. (1990). "Manual for estimating soil properties for foundation design." *Final Rep., EPRI EL-6800*, Electric Power Res. Power Inst., Pleasant Hill, Calif.

Lwin, M., and Henley, E. H. Jr. (1991). "Bridge seismic retrofit program report." *Bridge and Struct. Ofc. Rep.*, Washington State Dept. of Transp., Olympia, Wash.

O'Donovan, T. O., Eberhard, M. O., and Marsh, M. L. (1994). "Lateral-load response of two reinforced concrete bents." Tech. Rep. WA-RD 305.3, Washington State Dept. of Transp., Olympia, Wash.

O'Neill, M. W., and Murchison, J. M. (1983). "An evaluation of P-Y relationships in sands." *Rep. PRAC 82-41-1*, American Petroleum Institute, Houston, Tex.

Priestley, M. J. N., Seible, F., and Chai, Y. H. (1992). "Design guidelines for assessment, retrofit, and repair of bridge for seismic performance." *Rep. No. SSRP-92-01*, Dept. of Appl. Mech. and Engrg. Sci., Univ. of California, San Diego.

Roberts, J. E. (1991). "Research based seismic design and retrofit of California bridge." *Proc., 1st Annu. Seismic Res. Workshop*, California Department of Transportation, Sacramento, Calif., 1–10.

Rodehaver, S. M. (1993). "Dynamic testing and analysis of a reinforced concrete bridge," MS thesis, Dept. of Civ. Engrg., University of Washington, Seattle, Wash.

Wilson, E. L., and Habibullah, A. (1989). "SAP90 users manual." Computers and Structures, Inc., Berkeley, Calif.